Effect of molarity of TiO_2 seeded-template to the growth of ZnO nanostructures

N.A.M. Asib[1,2,a], A. N. Afaah[1,2], A. Aadila[1,2], M. R. Mahmud[1,2], Lim Y. C.[1], Salman A.H. Alrokayan[4], Haseeb A. Khan[4], M. Rusop[1,3], Z. Khusaimi[1,2,b]
[1]Faculty of Applied Sciences;
[2]NANO-SciTech Centre, Institute of Sciences;
[3]NANO-ElecTronic Centre, Faculty of Electrical Engineering;
Universiti Teknologi MARA, 40450 Shah Alam, Selangor, Malaysia
[4]Research Chair of Targeting and Treatment of Cancer Using Nanoparticles, Department of Biochemistry, College of Science, King Saud University, Riyadh, Saudi Arabia

E-mail: [b]zurai142@salam.uitm.edu.my, [a]amierahasib@yahoo.com

Abstract. ZnO nanostructures were deposited by solution-immersion method on TiO_2 layers by sol-gel spin-coating technique. Seven layers of TiO_2 were coated on glass substrates at different molarities, followed by annealing treatment and solution-immersion process in aqueous solution containing 1:1 ratio of 0.05 M of zinc nitrate hexahydrate ($Zn(NO_3)_2.6H_2O$) and hexamethylenetetramine (HMTA) ($C_6H_{12}N_4$). FESEM images confirmed that ZnO nanostructures grown on TiO_2 seeded-template are in needle-like shape with smaller tip can be observed. Photoluminescence (PL) spectroscopy showed that as the molarity of TiO_2 seeded-template increase, the intensity of PL emission at UV region decrease. UV emission peak for 0.10 M and 0.25 M are higher compared to UV emission peak film of 0.50 M and 1.00 M, which are too low. Meanwhile, the UV absorption properties of the nanostructured thin film for 0.25 M of TiO_2 seeded-template was higher compared to other thin films.

1. Introduction

In the field of semiconductor nanostructures, one–dimensional (1D) Zinc oxide (ZnO) nanostructures (e.g. nanowires, nanorods, nanobelts) becoming the most promising candidates due to their important physical properties and application prospects. ZnO is a direct band gap semiconductor with hexagonal wurtzite crystal structure, having good optical and electrical properties including has a wide band gap of 3.37 eV, large exciton binding energy about 60 meV and has high refractive index of 2.01 [1]. These excellent properties of ZnO thin films, have increase the interest of many researches to study about the material especially in nanoscale as the nanoscale electronic devices have the potential to achieve faster response and higher sensitivity compared to bulk material [2]. ZnO can be widely applied in various fields such as in optical and optoelectronic devices [3], photocatalysts, solar cell, UV light emitting diodes and UV sensor.

In ZnO based UV sensor, many efforts have been made to improve the performance of the devices. It is known that the performance of the device depends on the surface condition, structural quality and the dimension of ZnO nanostructures. Surface modification or structural improvement is expected can increase the sensor performance. Where, the process of modifying the surface is related to the surface adsorption of gas molecules from the atmosphere and surface defects, which influence the

characteristics of sensor [4]. Therefore, an approach of utilizing the catalytic seed layer to growth better ZnO was used as this seed layer can act as nucleation centres to prepare a suitable site to which ZnO nanostructures can adhere since it can provide an almost mistmach-free interfacial layer between the ZnO and the seed layer so that well aligned of ZnO nanostructures can grow. In addition, the seed layer can assits an epitaxial growth process on the seed layer coated on glass substrate.

Since titanium dioxide (TiO_2) is also a material that belongs to the group of metal oxide, it can be a good candidate of seed layer due to its excellent properties such as good semiconductor properties, high chemical stability, high photocatalytic activity, non-toxicity [5] and long thermal photostability [6]. Besides, TiO_2 has a wide direct band gap of 3.0 eV or 3.2 eV in the rutile or anatase crystalline phase which is similar to ZnO. However, ZnO is a direct band gap semiconductor but TiO_2 is an indirect band gap semiconductor with a relative lower cost [3, 7]. Moreover, TiO_2 can act as catalytic promoter during the involved reaction [8] and can greatly modified the physical and optical properties of thin films when we introduce it into ZnO matrices [9, 10].

Nanostructures of ZnO can be produced by several methods such as spray pyrolysis [11], chemical vapour synthesis (CVS) [12], pulsed laser deposition, and solution-based method. In particular, solution-based method has advantages of synthesizing nanostructured ZnO at low processing temperature and low cost. The simplicity of the experimental method of preparing a large-area thin film with excellent compositional control suitable for large-scale production of ZnO [13].

In this study, we prepared TiO_2 as a seeded-template for fabrication of ZnO nanostructures using sol-gel spin-coating and solution-immersion method, respectively. The effect of different molarities of TiO_2 as a seeded-template to the growth of ZnO nanostructures were investigated based on the changes of surface morphology and optical properties shown by the nanostructures thin films measured from Field Emission Scanning Microscope (FESEM), Photoluminescence (PL) spectroscopy and Ultraviolet-Visible (UV-Vis) spectrophotometer. These changes of properties are expected can improve the performances of cost-effective devices such as UV photoconductive sensor.

2. Experimental

2.1. Materials and chemicals

Glass substrate, Titanium (IV) butoxide, Ethanol, Triton-X-100, Glacial acetic acid (GAA), Zinc nitrate hexahydrate ($Zn(NO_3)_2.6H_2O$) and Hexamethylenetetramine ($C_6H_{12}N_4$) HMTA.

2.2. Preparation of TiO_2 seeded-template

Titanium (IV) butoxide was used as a starting material for TiO_2 seeded-template preparation. Prior to seed layer deposition, titanium (IV) butoxide dissolved in ethanol as solvent with triton-X-100 as stabilizer, under constantly stirring. Then, glacial acetic acid (GAA) within distilled water was added to the solution in order to accelerate the chemical reaction in the solution. The mixture was heated at 60 °C for 2 hours and left to aged for 24 hours with continuously stirring. To investigate the effect of different molarity of TiO_2 as seeded-template to ZnO nanostructures, molarity of TiO_2 solution were varied at 0.10, 0.25, 0.50 and 1.00 M. Coating layer of TiO_2 is performed by spin-coater at three steps of different speeds on a glass substrate, followed by drying process at 150°C for 10 minutes. For each layer, the same procedure was repeated until seven layers of coating. Finally, the TiO_2 seeded templates were annealed in annealing chamber for at 450 °C to crystallize the templates.

2.3. Preparation of needle-like ZnO

ZnO nanostructures were fabricated on TiO_2 seeded-template via solution-immersion method. Aqueous solution of zinc nitrate hexahydrate ($Zn(NO_3)_2.6H_2O$) was used as a precursor in 100 ml of deionized water. As a stabilizer, hexamethylenetetramine, HMTA ($C_6H_{12}N_4$) also was dissolved in 100 ml of deionized water and added to the Zn^{2+} solution with molar ratio 1:1. Then, another 50 ml of deionized water was added to increase the volume of the solution up to 250 ml. The solution was heated at 60 ^{0}C for 1 hour and left to aged for 24 hours at room temperature with continuous stirring.

The TiO_2 seeded-templates were suspended in centrifuged tubes which contained the prepared solution. The growth of ZnO nanostructures was take placed in water bath at 70-90 °C for 4 hours. After the deposition, the thin films were taken out and rinsed with deionized water several times, followed by annealing process at 500 ^{0}C for 1 hour

2.4. Characterization of TiO_2: ZnO nanostructures thin films

The change in surface morphology and optical properties between bare ZnO nanostructures and ZnO 7nanostuctures grown on different molarities of TiO_2 seeded-template were observed by using FESEM (JEOL JSM-7600F), PL spectroscopy (Horiba Jobin Yvon) and UV-Vis spectrophotometer (VARIAN 5000).

3. Results and discussion

3.1. Field emission scanning electron microscope (FESEM)

Figure 1 show FESEM images of the surface morphologies of needle-like ZnO nanostructures deposited on glass substrate without seed layer of TiO_2 (Figure 1 (a)) and with varied molarities of TiO_2 seed layer (Figure 1 (b-f)) that were fabricated via solution-immersion method. The images were captured at 5.0 kV of voltage at 10 kx magnification.

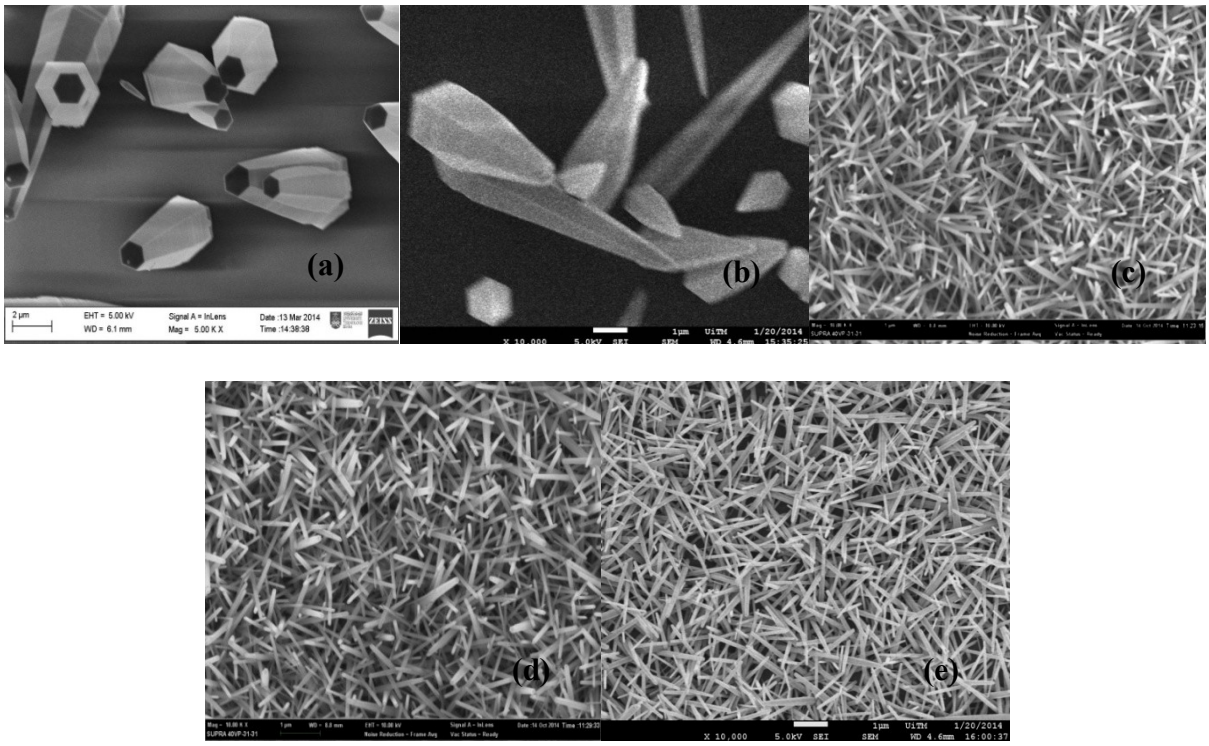

Figure 1. FESEM images of (a) bare ZnO and ZnO nanostructures deposited on (b) 0.10, (c) 0.25, (d) 0.50 and (e) 1.00 M of TiO_2 seeded-template.

Figure 1 (a) shows surface view images of ZnO nanostructures with hexagonal tip grown on glass substrate. As the TiO_2 seed layers were coated on the glass substrates, needle-like ZnO nanostructures with smaller tip can be seen on all the the TiO_2 templates, as shown in Fig. 1 (b) until Fig. 1 (e). It is revealed that the needle-like ZnO nanostructures are well grown with smaller diameter sizes and denser arrays on the TiO_2 coated-substrates compared to bare ZnO. Table 1 recorded the estimated average diameter of the needle-like ZnO nanostructures ranged between 61.2 nm to 1254.2 nm. A

magnified FESEM images of ZnO as shown in Figure 1 (a) clearly confirms that needle-like ZnO with bigger sizes and less dense arrays were deposited on glass substrate. As the molarity of TiO_2 seeded templates are increase to 1.00 M, the average diameter sizes of needle-like ZnO nanostructures are significantly change to smaller sizes with denser distribution of ZnO. For 0.25, 0.50 and 1.00 M of TiO_2, the average diameter sizes of ZnO were about 61.2, 61.3 and 62.5 nm, respectively with good distribution of ZnO. The smallest diameter size of needle-like ZnO nanostructures with most dense arrays was deposited on 0.25 M of TiO_2. At low concentration, smaller sizes of particles is formed [14]. The decreasing in sizes of TiO_2 contribute to the sizes reduction of ZnO nanostructures grown on this seed layer [15]. The densification of the TiO_2 particles resulted from smaller size of grown particles causes formation of compact particles thus, resulted more nanostructures of ZnO with smallest sizes appeared in the thin film compared to other samples as shown and recorded in Figure 1 (c) and Table 1.

Table 1. Average diameter size of bare ZnO and needle-like ZnO nanostructures deposited on different molarities of TiO_2 seeded-template.

Sample	Average diameter size of ZnO (nm)
ZnO	1254.2
TiO_2(0.10 M): ZnO	533.3
TiO_2(0.25 M): ZnO	61.2
TiO_2(0.50 M): ZnO	61.3
TiO_2(1.00 M): ZnO	62.5

3.2. Photoluminescence (PL) study

PL spectroscopy was used to investigate the optical properties and quality of bare ZnO and ZnO nanostructures grown on different molarities of TiO_2 seed layer. When excited under laser source of 325 nm, there are difference were observed between the PL spectrums corresponding to different conditions of ZnO fabrications as shown in Figure 2.

The narrow UV band which appeared due to free-exciton recombination by the process of exciton-exciton collison [3, 16] at 394 nm and broad visible band within the range 600- 666 nm are observed for bare ZnO which grown on glass substrate only, without coated with TiO_2 seed layer. Meanwhile, when the molarity of TiO_2 seeded-template increases from 0.10 M to 1.00 M, the UV band are blue shifted to the left compared to the bare ZnO thin film and the broad visible band are extending from 550- 700 nm. The position of the UV band for each samples were recorded in Table 2. The blue shifted of UV peak emission to the lower wavelength might be due to the reduction of ZnO nanostructures sizes and typically, visible band arises due to structural and surface defects such as zinc interstitials (Z_{ni}), oxygen vacancies (V_O), oxygen interstitials (O_i), Zn vacancies (V_{Zn}) and the oxide antisite defect (O_{Zn}) [17, 18]. As the molarity of TiO_2 seeded-template increases, obvious decreases of UV peak emissions intensity are observed. The intensity of UV emission peak for 0.10 M and 0.25 M are clearly seen and higher compared to 0.50 M and 1.00 M, which are too low. Thus, 0.10 M and 0.25 M has higher crystallinity of ZnO nanostructures due to free exciton emission [19].

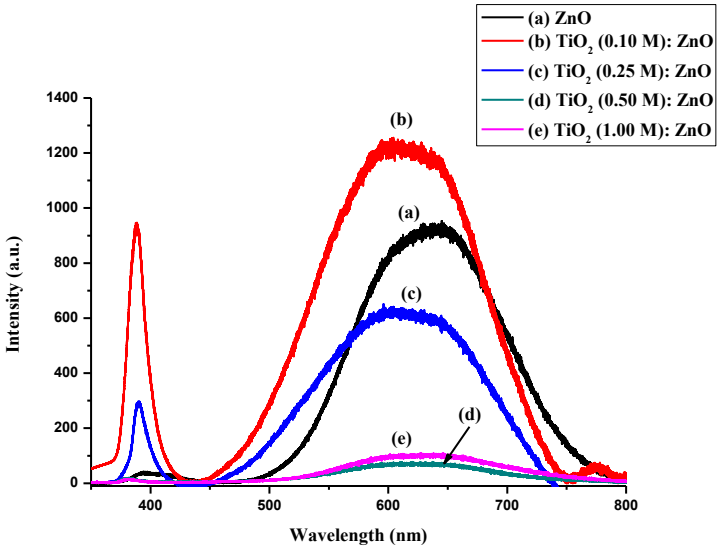

Figure 2. PL spectra of bare ZnO and ZnO nanostructures deposited on different molarities of TiO_2 seeded-template.

The crystal quality and optical properties are known to be enhanced when the ratio of UV emission peak intensity and the visible emission peak intensity, I_{UV}/I_{VIS} is increased [17, 20, 21]. The high peak intensity ratios indicates the decrease of defect concentrations and impurities in grown materials with the molarity decrease from 1.00 M to 0.10 M. The calculated ratio, I_{UV}/I_{VIS} were recorded to be 0.04, 0.76, 0.47, 0.26 and 0.14 for bare ZnO, 0.10, 0.25, 0.50 and 1.0 M of TiO_2 seeded-template, respectively as also recorded in Table 2. Therefore, the ZnO nanostructures grown on the TiO_2 seeded-template has better crystal and optical quality of the nanostructures thin films compared to bare ZnO.

Table 2. Position of UV emission peak and the ratio of the UV emission peak intensity and the visible emission peak intensity, I_{uv}/I_{vis} based on PL spectra for bare ZnO and ZnO nanostructures deposited on different molarities of TiO_2 seeded-template.

Sample	Wavelength of UV emission peak (nm)	I_{UV}/I_{Vis}
ZnO	395	0.04
TiO_2(0.10 M): ZnO	389	0.76
TiO_2(0.25 M): ZnO	390	0.47
TiO_2(0.50 M): ZnO	383	0.26
TiO_2(1.00 M): ZnO	383	0.14

3.3. Ultraviolet-visible (UV-Vis) study

Figure 3 displays the UV-Vis spectrum for bare ZnO and TiO_2: ZnO nanostructures thin films, at four different TiO_2 percursor concentrations (0.10, 0.25, 0.50 and 1.00 M). The fabricated TiO_2: ZnO nanostructures thin films show good transparency in the visible region (400-800 nm) and high absorption properties at UV region (below 400 nm).

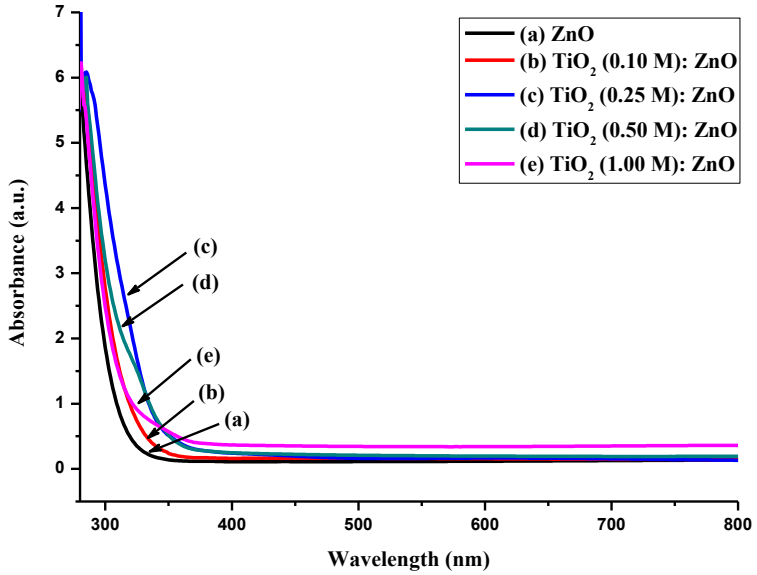

Figure 3. UV-vis absorbance spectra of bare ZnO and ZnO nanostructures deposited on different molarities of TiO_2 seeded-template.

In a comparison to bare ZnO, the ZnO nanostructures grown on TiO_2 seeded-template exhibit stronger absorption properties in UV and visible region. This can be attributed to the improvement of light-harvesting efficiency, which enhance the use of UV light compared with bare ZnO [22, 23]. It is suggested that the improvement are likely due to the existence of TiO_2 that modifies the ability of the samples in efficiently adsorbed the incident light reaching the thin films. This improvement also indicates the reduction in transmittance of the thin films and might be resulted from the trapped incident lights caused by scattering in the needle-like structure [18]. As seen in the FESEM images, needle-like ZnO nanostructures have denser distribution as the molarities of TiO_2 increase. The increasing of grown ZnO which were distributed vertically and horizontally towards the TiO_2 nanoparticles surface caused increasing of trapped incident light in the thin films. Hence, the optical path length inside the thin films might also increase and improved the light absorption. The red shift was observed on the absorption edges of the TiO_2: ZnO nanostructures compared to the ZnO thin film. The light scattering and the grain size of one-dimensional nanostructure might have influenced this red shift in longer-wavelength region [22].

For bare ZnO, although the thin film has weak UV absorption properties, it means that the sample has good transmittance which higher at both regions, UV and visible regions (300- 800 nm). This reason might be resulting from the smoother surface morphology and less grain boundaries of the thin film has, as confirmed by FESEM result above. From Figure 1 (a), bare ZnO thin film has less dispersion which contributes to the lower distribution of fabricated needle-like ZnO on the glass substrate and thus leads to the lower grain boundary. When the incident light scattered on the smoother surface with less denser distribution of needle-like ZnO, more light can escaped and passed through the thin film and caused higher optical transmittance values [24, 25].

4. Conclusion

ZnO nanostructures were successfully synthesized via solution-immersion method on TiO_2 seeded-template prepared by sol-gel spin-coating technique, on the glass substrates. FESEM images revealed

that needle-like ZnO nanostructures with smaller tip can be seen on the templates as the TiO_2 seed layers were coated on the glass substrates. From PL spectra, when the molarity of TiO_2 seed layer increases from 0.10 M to 1.00 M, the UV band are blue shifted to the left compared to the bare ZnO nanostructures thin film and the broad visible band are extending from 550- 700 nm. The blue shifted of UV peak emission to the lower wavelength might be due to the reduction of ZnO nanostructures sizes. Besides, ZnO nanostructures grown on the TiO_2 seeded-template has better crystal and optical quality of the nanostructures thin films compared to bare ZnO. Furtherrmore, in a comparison to bare ZnO, the ZnO nanostructures grown on TiO_2 seeded-template exhibit stronger absorption properties in UV and visible region which was likely improved the light-harvesting efficiency of the thin films. As a result, ZnO nanostructures grown on 0.25 M of TiO_2 seeded-template, having smallest average size of ZnO nanostructures, better crystallinity, improved optical quality and high UV absorption properties might be promising for use in UV photoconductive sensor. Future work in observing the influence of number of TiO_2 layers to the grown ZnO nanostructures should be done for further investigation.

5. Acknowledgement

We would like to express our gratitude to Ministry of Education Malaysia and Research Management Institute, Universiti Teknologi MARA (UiTM), Shah Alam, Selangor, Malaysia and Long-Term Research Grant Scheme for Nanostructures, Nanomaterials and Devices for Fuel Cells and Hydrogen Production (600-RMI/LRGS 5/3 (3/2013)) for the financial support. This study was also supported by the Research Chair of Targeting and Treatment of Cancer Using Nanoparticles, Deanship of Scientific Research, King Saud University, Riyadh, Saudi Arabia.

6. References

[1] C.-C. 2012 *Nanorods* (Croatia: InTech) pp 33-50.
[2] P. K. G. Soumen Dhara 2012 *Nanorods* (Croatia: InTech) pp 1-32.
[3] T. A. Yinyan Gong, Gertrude F. Neumark, Stephen O'Brien, and Igor L. Kuskovsky 2007 *Nanoscale Res Lett.* **2** 297
[4] Z. K. Mohamad Hafiz Mamat, Musa Mohamed Zahidi and Mohamad Rusop Mahmood, O. Yalçın 2012 *InTech*. 250.
[5] S. T. Jirapong Arin and Titipun Thongtem 2013 *Materials Letters* **96** 78
[6] Baoshun Liu, Qi Hu Liping Wen, and Xiujian Zhao 2009 *Thin Solid Films* **517** 6569
[7] Hua-Jie Wang, Yuan-Yuan Sun, Ying Cao, Xue-Hong Yu, Xiao-Min Ji and Lin Yang 2011*Chemical Engineering Journal* **178** 8
[8] E. C. Davide Barreca, Angelo P. Ferrucci, Alberto Gasparotto, Chiara Maccato, Cinzia Maragno, Giorgio Sberveglieri, and Eugenio Tondello 2007 *Chem. Mater* **19** 5642
[9] Simin Janitabar-Darzi and Ali Reza Mahjoub 2009 *Journal of Alloys and Compounds* **486** 805
[10] M. A. Kanjwal, N. A. M. Barakat, F. A. Sheikh, S. J. Park, and H. Y. Kim 2010 *Macromolecular Research* **18** 233
[11] Bambang Veriansyah, Jae-Duck Kim, Byoung Koun Min, Young Ho Shin, Youn-Woo Lee, and Jaehoon Kim 2010 *J. of Supercritical Fluids* **52** 76
[12] F. A. A. Guvenc Akgul, Klaus Attenkofer, Markus Winterer 2013 *Journal of Alloys and Compounds* **554** 177
[13] S. A. Z. Khusaimi, H. A. Rafaie, M. H. Mamat, N. Abdullah, S. Abdullah, M. Rusop 2009 *Malaysian Journal of Science 28 (Special Edition)* **28** 197
[14] M. N. b. A. Mohd Faizal b Achoi, Mohamad Rusop, and Saifollah Abdullah 2011 *Transaction of the Materials Research Society of Japan* **36** 273.
[15] A. A. N.A.M. Asib, A.N. Afaah, M. Rusop, and Z. Khusaimi 2014 *Advanced Materials Research* **832** 596
[16] D. Basak, G. Amin, B. Mallik, G. K. Paul, and S. K. Sen 2003 *Journal of Crystal Growth* **256** 73

[17] Q. L. Zi Qin, Yunhua Huang, Lidan Tang, Xiaohui Zhang, and Yue Zhang 2010 *Materials Chemistry and Physics* **123** 811
[18] Z. K. M.H. Mamat, M.Z. Musa, M.F. Malek, and M. Rusop 2011 *Sensors and Actuators A: Physical* **171** 241
[19] A. A. F.S. Husairi, M. Rusop, and S. Abdullah 2013 *Microelectronic Engineering* **108** 145
[20] J. Lee, JooyoungChung, and SangwooLim 2010 *Physica E* **42** 2143
[21] M. H. Mamat, Z. Khusaimi, M. M. Zahidi, and M. R. Mahmood 2011 *Japanese Journal of Applied Physics* **50**
[22] J. T. Hong Zhu, Tao Wang and Jie Deng 2011 *Applied Surface Science* **257** 10494
[23] A. A. Chun Cheng, Chao Zhu, Zuli Xu, Haisheng Song and Ning Wang 2014 *Scientific Reports*
[24] C. M. Firdaus, M. S. B. S. Rizam, M. Rusop, and S. R. Hidayah 2012 *Procedia Engineering* **41** 1367.
[25] Prabitha B. Nair, V.B.Justinvictor, Georgi P.Daniel, K.Joy, V.Ramakrishnan, and P.V.Thomas 2011 *Applied Surface Science* **257** 10869